

AN ACCURATE DISTANCE TO HIGH-VELOCITY CLOUD COMPLEX C

C. THOM^{1,2}, J.E.G. PEEK³, M.E. PUTMAN⁴, CARL HEILES³, K.M.G. PEEK³, R. WILHELM⁵*Draft version May 18, 2019*

ABSTRACT

We report an accurate distance of $d = 10 \pm 2.5$ kpc to the high-velocity cloud Complex C. Using high signal-to-noise Keck/HIRES spectra of two horizontal-branch stars, we have detected Ca II K absorption lines from the cloud. Significant non-detections towards a further 3 stars yield robust lower distance limits. The resulting H I mass of Complex C is $M_{\text{HI}} = 4.9_{-2.2}^{+2.8} \times 10^6 M_{\odot}$; a total mass of $M_{\text{tot}} = 8.2_{-2.6}^{+4.6} \times 10^6 M_{\odot}$ is implied, after corrections for helium and ionization. We estimate the contribution of Complex C to the mass influx to be $\sim 0.1 M_{\odot} \text{ yr}^{-1}$.

Subject headings: Galaxy: halo — Galaxy: evolution — ISM: clouds — ISM: individual (Complex C)

1. INTRODUCTION

The halo of the Milky Way contains clouds of neutral hydrogen (H I) gas representing the flow of baryons into, and out of, the Galactic disk. Identified by their velocities, these high-velocity clouds (HVCs)⁶ have been observed in H I 21cm emission for more than 40 years (Muller et al. 1963). Since their distances cannot be determined by the application of a kinematic model, the mass scale of the flow is uncertain and the clouds' origin and impact on the disk open to speculation.

Since their discovery, many explanations have been offered for the HVC phenomenon, with a corresponding range of distances; most of these explanation can be traced to Oort (1966). Currently favored suggestions for the origin of HVCs include supernovae-driven Galactic fountains, in which gas is expelled from the disk into the halo, condenses and then returns in a cyclic flow (Bregman 1980; Houck & Bregman 1990). There is evidence that some (but not all) of the extraplanar H I observed in edge-on spiral NGC 891 originates in such a fountain (Oosterloo et al. 2007). Theoretical models suggest fountain gas may rise as high as ~ 10 kpc above the disk (de Avillez 2000). Dwarf galaxy accretion is another avenue for mass input; the well-known Magellanic Stream (Mathewson et al. 1974; Putman et al. 2003) is the canonical example, but this mechanism has been suggested for other MW satellites (Putman et al. 2004). Another recent proposal posits the clouds to be condensing out of the hot MW halo (Maller & Bullock 2004; Kaufmann et al. 2006; Sommer-Larsen 2006; Peek et al. 2007), at a range of distances up to ~ 150 kpc. Peek et al. (2007) suggested that HVC masses are inversely proportional to their distance,

reasoning that condensing clouds are small at large distance, and form the seeds of the large HVC complexes, into which they grow via accretion as they approach the disk. If this scenario is correct, then all the large HVC complexes would be close ($d \sim 10 - 15$ kpc).

Complex C was first mapped by Hulsbosch & Raimond (1966). Its large angular size ($\sim 1600 \text{ sq. deg.}$) means that a number of UV-bright quasars align with high column-density gas, allowing metallicity determinations by absorption line spectroscopy. Based on a metallicity measurement of $\sim 0.1 Z_{\odot}$, Wakker et al. (1999) suggested Complex C is a low-metallicity, infalling cloud, fueling Galaxy formation. Gibson et al. (2001) later reported metallicities as high as $0.3 Z_{\odot}$, suggesting that Complex C is instead a product of star formation in the Galaxy. Most recently Collins et al. (2007) confirmed this evidence of abundance variations across the cloud independent of ionization effects, suggesting the possible mixing of primordial and enriched gas (see also Tripp et al. 2003).

There is no convincing evidence of dust in Complex C (e.g. Collins et al. 2003), nor any detections of molecular hydrogen (Murphy et al. 2000; Richter et al. 2001). Observations with the Wisconsin H α Mapper (WHAM) have detected H α emission at the same velocities as the H I emission (Tuftte et al. 1998; Haffner et al. 2003). Higher ionization species, such as C IV, Si IV, N V and O VI have been seen in absorption towards QSOs (Sembach et al. 2003; Fox et al. 2004). Fox et al. (2004) studied the O VI and other highly ionized species, concluding that they are most likely to arise in conductive or turbulent interface regions between the warm neutral gas seen in H I, and the surrounding hot halo medium.

HVCs are often invoked by Galactic chemical evolution models as a source of infalling star formation fuel, which is needed in order to reproduce the metallicity distribution function of stars in the solar neighborhood (the “G Dwarf” problem; e.g. Pagel & Patchett 1975; Alibés et al. 2001). As the largest HVC on the sky, Complex C could potentially contribute a significant fraction of the Galaxy's future star formation fuel. For HI clouds, the mass is related to the distance by $M_{\text{HI}} = 0.236 S d^2$, where S is the total H I flux observed (in Jy km s^{-1}) and d the distance in kpc. For Complex C, $S = 2 \times 10^5 \text{ Jy km s}^{-1}$ (Wakker & van Woerden

Electronic address: cthom@uchicago.edu

¹ Department of Astronomy and Astrophysics, University of Chicago, Chicago, IL, 60637, USA² Kali Institute for Cosmological Physics, University of Chicago, Chicago, IL, 60637, USA³ Astronomy Department, University of California, Berkeley CA, 94720, USA⁴ Department of Astronomy, University of Michigan, Ann Arbor, MI 48109, USA⁵ Department of Physics, Texas Tech University, Lubbock, TX 79409, USA⁶ HVCs are defined as having $|v_{\text{LSR}}| > 90 \text{ km s}^{-1}$ and hence do not co-rotate with the Galaxy.

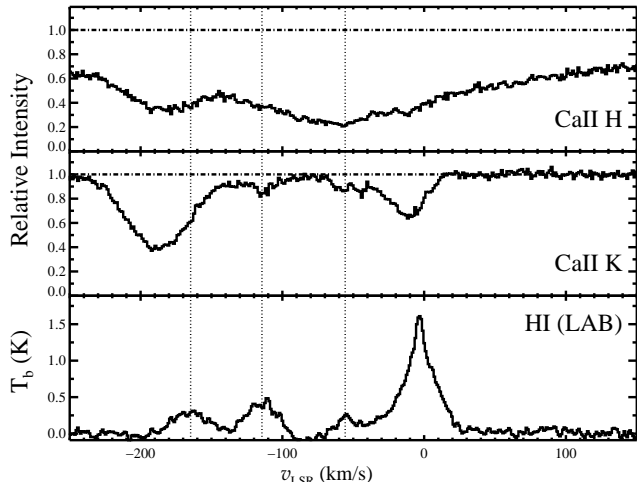


FIG. 1.— S437: Detection of Complex C in absorption towards S437. In this direction, we see the HVC in emission at $v_{\text{LSR}} = -115 \text{ km s}^{-1}$, which is clearly seen in Ca II K absorption. There is also a higher velocity component seen in emission (sometimes called the “high-velocity ridge”) at $v_{\text{LSR}} = -165 \text{ km s}^{-1}$. This higher-velocity component is not detected, since HVC Ca II K absorption is obscured by the stellar Ca II K line, and the Ca II H line is obscured by both core of the stellar H ϵ line and the stellar Ca II H absorption. IVC gas is evident at $v_{\text{LSR}} = 56 \text{ km s}^{-1}$.

1991). Here we use stellar absorption to determine the most accurate measurement of d for Complex C to date.

2. DATA

Five horizontal branch stars from the catalogue of Sirko et al. (2004) that align with Complex C were observed with the Keck/HIRES telescope and instrument combination on 08 June 2007 and 09 June 2007 (UT). We employed the UV cross-disperser to maximize throughput at Ca II K ($\lambda 3933.663$), and binned the data $2\times$ in the spatial direction. In this configuration, the Na I D lines are within our wavelength coverage, but are at the extreme edge of the order, and do not add substantial information. The $7'' \times 0.8''$ slit yielded a resolution of $R \sim 48,000$. Over the course of the two nights, the seeing varied from $\sim 1.2 - 1.8''$, but we nevertheless obtained excellent quality data. Table 1 summarizes our targets. For these stars, stellar parameters were obtained using the techniques described in Wilhelm et al. (1999). Absolute magnitudes and distances for the stars were determined by comparing T_{eff} , $\log g$, and $[\text{Fe}/\text{H}]$ to the run of theoretical isochrones of Girardi et al. (2004) and Dorman (1992); distances are given in the text, and in Table 2. External tests of the stellar technique against stars in globular clusters indicate that distances are accurate to $\sim 25\%$ (Wilhelm et al. 2008, in prep.). We thus adopt a 25% error as our formal distance error; in all cases this error is greater than that estimated from the stellar classification, sometimes significantly. Continuing calibration efforts of the Segue Stellar Parameter Pipeline (Lee et al. 2008) should improve this accuracy in the future.

To reduce the data, we used the HIRES Redux pipeline that is part of the *xidl* package⁷ (Bernstein, Burles & Prochaska, 2008, in prep.). The package applies standard

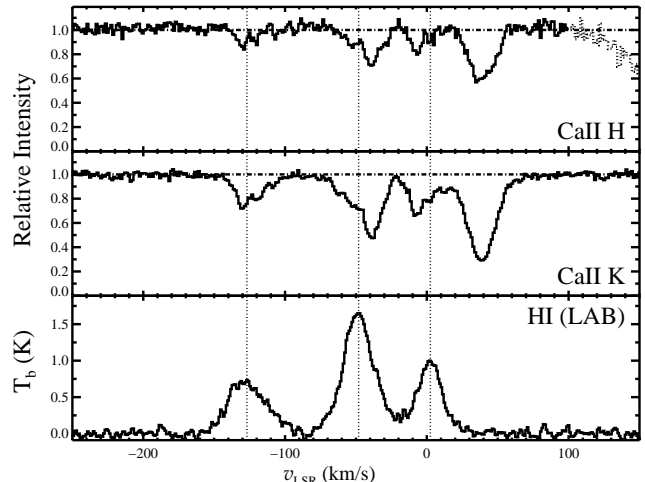


FIG. 2.— S674: Strong absorption from Complex C is evident at -127 km s^{-1} , setting an upper distance limit. Intermediate-velocity absorption from the IV-arch can also be seen at -48 km s^{-1} . See text for further details.

bias and flat-field corrections, performs a 2-D wavelength calibration, and extracts the individual orders to give final 1-D spectra and associated errors. For equivalent width measurements, we fit the local continuum with a low-order Legendre polynomial and directly integrate the data, determining error contributions from both the noise and continuum fitting (Sembach & Savage 1992). In general, the HVC Ca II H ($\lambda 3968.467$) line is in the wings (and in some cases in the core) of the broad stellar H ϵ ($\lambda 3970.072$) line. The H ϵ line is sufficiently broad that it completely dominates the echelle order, and the true continuum cannot accurately be determined. Since we care only about the HVC Ca II H line, we fit a pseudo-continuum along the balmer line wing where possible, removing its contribution to the absorption.

HI spectra were primarily drawn from the combined Leiden/Argentine/Bonn (LAB) survey, which has a beam-width of $\sim 36'$ (FWHM) (Kalberla et al. 2005). In one case (S441—see Table 1), an H I spectrum from Effelsberg ($9'$ beam) is available. Heliocentric radial velocities (RVs) for all 5 stars were determined by fitting the positions of unblended metal lines in the echelle data. These are also given in Table 1. In most cases ~ 30 or more lines were available, but for S139, only 12 unblended metal lines are available in our Keck spectrum. Errors on RVs are the 1σ gaussian dispersion of the ensemble of measured lines.

Using the absorption line technique, upper or lower distance limits are placed on the distance to the HVC gas based on the detection or non-detections of absorption lines due to the gas, in the spectrum of stars at known distance. The technique is described in detail elsewhere (Schwarz et al. 1995; Thom 2006); Figure 1 of Schwarz et al. (1995) is particularly enlightening. Since the stars must lie at known (or knowable) distances, horizontal-branch and RR-Lyra stars are the most commonly used, but in principle any hot star at known distance may be used. In order to maximize the probability of optical detection, strong resonance transitions are the most appropriate. In the optical, Ca II H & K are the most common, but the Na I D lines may also be used

⁷ <http://www.ucolick.org/~xavier/IDL/index.html>

TABLE 1
JOURNAL OF OBSERVATIONS

Target	l (deg)	b (deg)	g_0 (mag)	S/N	v_{helio} (km s $^{-1}$)	Dist (kpc)	Label
SDSS J173424.01+601735.3	89.1	32.8	15.9	60	-482.6 ± 1.4	12.8 ± 3.2	S135
SDSS J172009.78+612502.3	90.6	34.4	14.7	100	-322.3 ± 3.3	7.8 ± 2.0	S139
SDSS J150335.53+623513.5	100.7	48.4	15.6	60	-201.2 ± 2.5	11.3 ± 2.8	S437
SDSS J153915.24+575731.7	91.2	47.5	15.9	80	-14.4 ± 1.5	10.2 ± 2.6	S441
SDSS J133654.82+622241.5	114.0	54.0	15.4	65	26.5 ± 0.9	10.4 ± 2.6	S674

NOTE. — SDSS names are created from the RA and DEC of the object, truncating co-ordinates. Galactic co-ordinates have been rounded to 0.1° . Magnitudes are extinction corrected g -band, taken from the SDSS database. Signal-to-noise measures are given for the continuum region near Ca II K. For convenience, we label each star with a number, corresponding to its numerical position in the catalogue of Sirko et al. (2004).

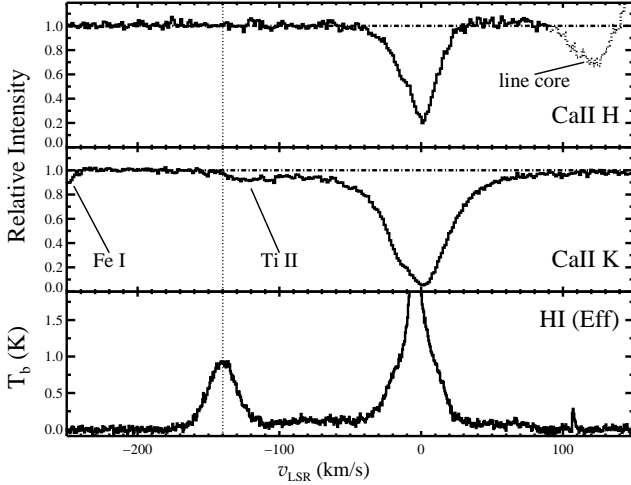


FIG. 3.— S441: No HVC absorption is present in the sightline towards S441. The weak feature in Ca II K red-ward of the HVC position is stellar Ti II. The dotted section in the Ca II H profile marks the core of the H ϵ balmer line, where the continuum fit is unreliable. The error spectrum is shown at the bottom of the top panel. Bottom panel shows the residuals of the fit. See text for details.

(see e.g. Thom et al. 2006). Strong UV transitions such as O I have also been used (Danly et al. 1993), and with the scheduled installation of the Cosmic Origins Spectrograph on the upcoming HST servicing mission, Mg II may also prove useful.

3. RESULTS

In the following, we discuss the individual lines of sight first for the detections (upper distance limits), then for the non-detections (lower distance limits). Refer to Table 2 for a summary of results and to Figure 7 for an H I column-density map with the positions of the stellar probes.

3.1. Upper Limits

S437, $d \sim 11$ kpc—Towards the star S437 two HVC emission components can be seen in the HI spectrum available from the LAB survey (Figure 1), at $v_{\text{LSR}} = -115$ km s $^{-1}$ and $v_{\text{LSR}} = -165$ km s $^{-1}$, with corresponding column densities $N(\text{H I}) = 2.1 \pm 0.3$ and $N(\text{H I}) = 1.5 \pm 0.4$ ($\times 10^{19}$ cm $^{-2}$). The HVC emission component at -115 km s $^{-1}$ is clearly evident in absorption at Ca II K, but the corresponding Ca II H line is lost in the core of

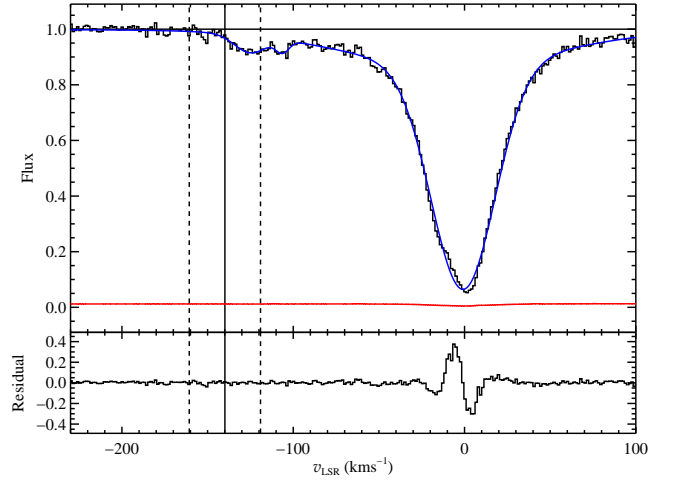


FIG. 4.— Fit to the stellar absorption in S441. The solid vertical line marks the expected HVC position. Dotted lines show the $\pm 2\sigma$ velocity range derived from the H I spectrum. See text for details.

the H ϵ balmer line. Since the HVC feature falls in the very core of the H ϵ line, we do not attempt to fit the continuum to the balmer line wings. The HVC component at -165 km s $^{-1}$ is lost in the strong stellar Ca II lines. Emission and absorption at $v_{\text{LSR}} = -56$ km s $^{-1}$ from the intermediate-velocity cloud (IVC) known as the “IV-arch” can also be seen. This cloud is known to be nearby ($0.4 < z < 3.5$ kpc; Ryans et al. 1997).

S674, $d \sim 10$ kpc—The optical spectra of S674, shown in Figure 2, provides a second detection towards the high latitude part of Complex C. Absorption is detected from Complex C at $v_{\text{LSR}} = -127$ km s $^{-1}$ setting an upper distance limit. We also detect the nearby IV-arch at $v_{\text{LSR}} = -48$ km s $^{-1}$, and the MW disk in absorption. Note that we have fitted the Ca II H continuum along the wing of the stellar H ϵ balmer line, removing it from Figure 2. The fall-off in the continuum red-ward of $v_{\text{LSR}} = 100$ km s $^{-1}$ in the Ca II H line is where the balmer line transitions from wing to core; since we use only a low order polynomial, and do not attempt to match the entire balmer line profile, the fit breaks down in this region.

We clearly detect multiple absorption components in the optical spectra which do not always align well with the H I emission positions. This is present in both the HVC absorption, as well as the IVC and disk gas. Since the H I data sample $36'$ on the sky, while the optical data

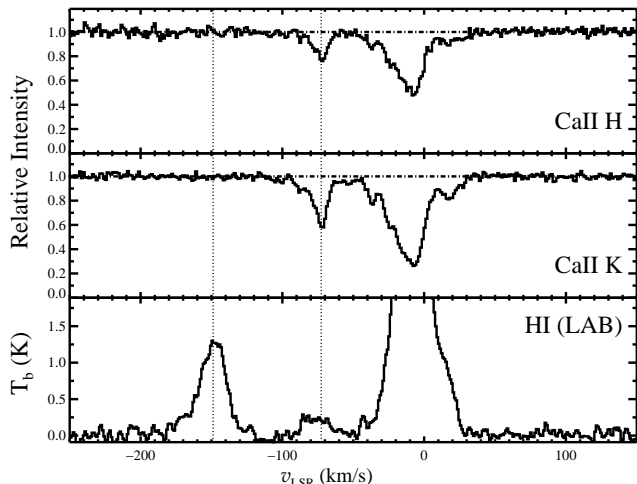


FIG. 5.— S135: No HVC absorption is evident at the expected velocity $v_{\text{LSR}} = -150 \text{ km s}^{-1}$. Multi-component IVC absorption can clearly be seen in both Ca II H & K absorption and H I emission. The strongest absorption component is at $v_{\text{LSR}} = -77 \text{ km s}^{-1}$. Galactic absorption components, seen in both Ca II K and Ca II H, are visible between $-40 \lesssim v_{\text{LSR}} \lesssim 20 \text{ km s}^{-1}$, corresponding to the strong H I emission.

trace a pencil beam, this may be a consequence of beam smearing. An interferometer map would be required to confirm this. Note, however, that in all cases, the optical absorption falls within the line limits defined by the H I data.

3.2. Lower Limits

S441, $d \sim 10 \text{ kpc}$ —At roughly the same latitude as our two detections, and only $\sim 28'$ from the Mrk 290 sightline, this line of sight has the most complicated optical spectrum. Figure 3 shows both the optical and radio spectra. Note that for this sightline, the H I spectrum comes from the Effelsberg telescope, which has a substantially smaller beam than the coarse resolution of the LAB survey.

The optical data in the Ca II K region show an absorption line slightly to the red ($v_{\text{LSR}} = -125 \text{ km s}^{-1}$) of where we expect the HVC absorption to lie ($v_{\text{LSR}} = -140 \text{ km s}^{-1}$). This line is *not* HVC absorption, but rather a Ti II line at a rest wavelength of 3932.020 \AA (Meggers et al. 1976). This identification is made based on several factors. Firstly, in the stellar rest frame, a fit to this line gives a rest wavelength 3932.00 \AA . This differs from the expected position by only 1.6 km s^{-1} , in good agreement with the measured radial-velocity precision (1.4 km s^{-1}). Second, the strength of this line is consistent with other Ti II lines in the spectrum of S441 with similar ionization potential and $\log gf$. Finally, the strength of this line is $W_\lambda = 25.9 \pm 1.4 \text{ m\AA}$. If this was an HVC Ca II K absorption line that was offset from the H I position, we would easily detect this line in the Ca II H transition [$\sigma(W_\lambda) = 2.5 \text{ m\AA}$]. We can thus exclude this possibility.

Since the stellar Ti II line only impinges on the wing of the expected HVC Ca II K absorption, and is very well fit by a single gaussian component, it does not diminish our ability to detect any putative HVC absorption line. Figure 4 shows the result of this fit. We include the

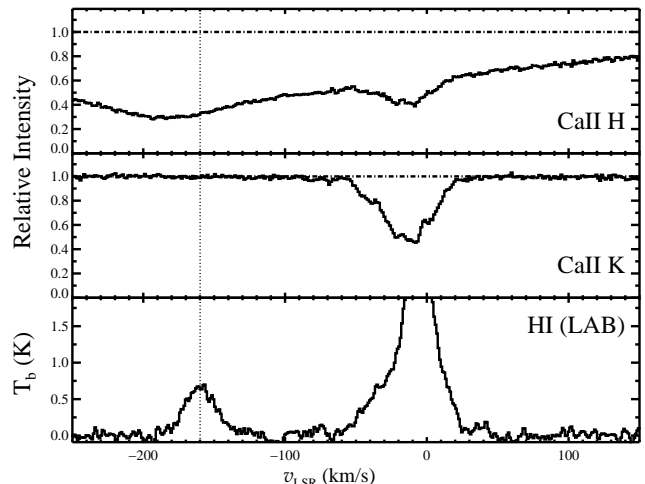


FIG. 6.— S139: No Ca II K absorption can be seen corresponding to the HVC emission at $v_{\text{LSR}} = -160 \text{ km s}^{-1}$. The Ca II H line falls in the core of the stellar H ϵ line.

strong stellar Ca II K line, and a very weak unidentified line at rest wavelength 3932.25 \AA ($v_{\text{LSR}} = -106 \text{ km s}^{-1}$). Both these latter features are well outside the region of interest for HVC absorption. The lower panel shows the residual of the fit. The expected HVC position is marked by the solid line, while the dotted lines mark the $\pm 2\sigma$ line width limits (where σ is the gaussian width of the H I spectrum). We emphasize that only the high quality of our Keck data allows us to cleanly remove the stellar absorption from the wing of the putative HVC region, and place a significant lower distance limit on the cloud.

Since the S441 sightline is very close to the Mrk 290 sightline, this significantly strengthens the conclusions that can be drawn from the non-detection of both Ca II K and Ca II H, since we can be confident of the level of HVC absorption expected. The worst-case expected HVC absorption toward this line of sight is 38 m\AA (Ca II K) and 19 m\AA (Ca II H); both these would be clearly visible. § 3.3 contains further discussion on the interpretation of non-detections.

S135, $d \sim 13 \text{ kpc}$ —The two stellar probes, S135 and S139 are both a few degrees from the edge of Complex C (See Figure 7), at lower latitude than our earlier targets. For S135, our most distant target, we see no indication of HVC absorption, as shown in Figure 5. Unrelated IVC gas can clearly be seen in both H I emission and absorption at $v_{\text{LSR}} = -77 \text{ km s}^{-1}$ in both Ca II H & K. This IVC gas can be seen in the LAB data cube to connect smoothly with the Galactic plane at lower latitudes. Although it is not shown in Figure 5, we also see this IVC in the Na I D₂ line, which is the stronger of the two Na I D doublet lines. The lack of HVC absorption sets a lower distance limit of $12.8 \pm 3.2 \text{ kpc}$.

S139, $d \sim 8 \text{ kpc}$ —The optical spectra of S139 are our highest signal-to-noise data. Figure 6 shows that there is clearly no absorption detected corresponding to the strong HVC emission. The Ca II H position is at the very core of the H ϵ balmer line, but the Ca II K data set a firm lower distance limit if $7.8 \pm 2.0 \text{ kpc}$. The Galactic emission shows a broad emission wing to $v_{\text{LSR}} \sim -50 \text{ km s}^{-1}$; Ca II K absorption components are also seen in this range. There is some evidence of IVC emission, with

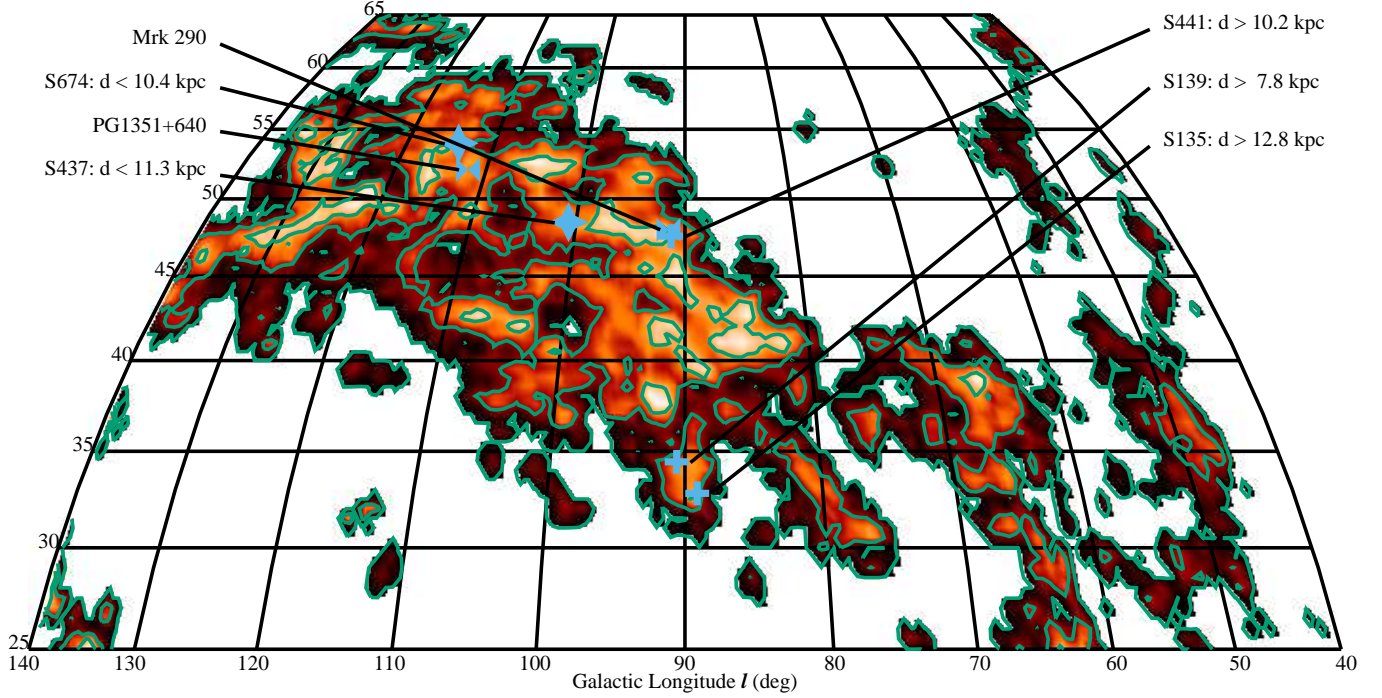


FIG. 7.— Location of SDSS stellar targets with respect to H I emission of Complex C. Contours are drawn at $\log N(\text{H I}) = 18.2, 19.0, 19.7$.

corresponding very weak absorption, in the range $v_{\text{LSR}} = 70 - 100 \text{ km s}^{-1}$, but better data are needed to confirm this. The lack of HVC absorption sets a lower distance limit.

3.3. Summary

Figure 7 shows the H I column density map of Complex C in Galactic co-ordinates, using an orthogonal projection. Contours are drawn at $\log N(\text{H I}) = 18.2, 19.0, 19.7$. The stellar lines of sight are marked with star symbols in the case of detections, and crosses in the case of non-detections. The stars are labeled (stars for detections, crosses for non-detections), along with the corresponding stellar distances. We also mark the position of the Mrk 290 and PG 1351+640 sightlines (hour-glasses), along which the Ca II abundance is measured, and we use to interpret our non-detections.

Towards the highest longitude stars—S437 and S674—we have detected Complex C in absorption, providing solid upper distance limits. Our remaining three targets show no evidence of HVC absorption. Table 2 provides a summary of these results. Stellar distances and measured H I column densities are given in Cols (2) and (3). Col (4) gives the predicted Ca II K equivalent width, based on the measured $N(\text{H I})$ and known Ca II abundance. Col (5) shows the worst-case equivalent width, assuming all factors work against us (see below). Col (6) gives the measured Ca II K equivalent width, or the 1σ error for non-detections. The significance of the result is indicated in Col (7). The final column listing the measured Ca II abundance, $N(\text{Ca II})/N(\text{H I})$, in the case of detections, or the assumed abundance in the case of non-detections (Wakker et al. 1996; Wakker 2001).

Non-detections are harder to interpret than detections; one must be convinced that the lack of absorption is not

a random confluence of bad luck. In general, one predicts the strength of the absorption that should be seen if the star is behind the gas, and shows that the data are of sufficient quality as to clearly detect absorption lines of that strength. Wakker (2001) has argued that one should adopt a worst-case scenario to interpret non-detections; in this view, it is not merely enough that the expected absorption be significantly stronger than the detection level, but we should account for the case in which every factor works against a detection. For example, the gas-phase abundance may be lower than expected, the column density may be lower than expected, and so on. This is quantified in the notion of multiplicative “safety factors”, which are given for a range of effects (Wakker 2001). The predicted absorption strength is reduced by this factor to obtain a worst-case absorption strength; only cases in which the noise level is less than this worst-case are deemed “strong” or significant non-detections.

Our H I column densities are mostly taken from the LAB survey, which samples $36'$ of sky, or Effelsberg ($9'$), both of which compare poorly to the pencil beam of the optical data. This may be clearly seen, for example, in the spectra of S674 above (Figure 2). Systematic uncertainties are therefore likely to be present since the radio and optical spectra sample different areas on the sky. Wakker et al. (2001) considered in detail the H I column-density derived with different sized beams, based on measurements at $36'$, $9'$, $1-2'$ and UV Ly α measurements. They conclude that a $36'$ beam gives a column density accurate to a factor of 3, which we adopt for the LAB data; Wakker (2001) suggests a factor of 2 for HI data with $9'$ resolution, which we use for S441 where Effelsberg data are available. We caution that variations may be still greater in cloud cores (Wakker et al. 2002) and we are pursuing interferometer data with Allen Tele-

TABLE 2
SUMMARY OF RESULTS

Target	Dist (kpc)	$N(\text{H I})$ ($\times 10^{19} \text{ cm}^{-2}$)	$W_{\lambda, \text{pred}}$ (mÅ)	Saf	$W_{\lambda, \text{saf}}$ (mÅ)	$W_{\lambda, \text{obs}} \pm \sigma(W_{\lambda})$ (mÅ)	Sig	$N(\text{Ca II})/N(\text{H I})$
Detections								
S437	11.3 ± 2.8	2.1 ± 0.3	37.3	46.9 ± 2.0	23	$26 \pm 4 \times 10^{-9}$
S674	10.4 ± 2.6	4.0 ± 0.5	72.1	76.5 ± 1.8	42	$22 \pm 3 \times 10^{-9}$
Non-detections								
S135	12.8 ± 3.2	4.9 ± 0.4	88.8	18	4.9	± 1.6	3.1	21.0×10^{-9}
S139	7.8 ± 2.0	3.3 ± 0.4	60.2	18	3.3	± 1.1	3.0	21.0×10^{-9}
S441	10.2 ± 2.6	4.2 ± 0.2	75.3	2	37.7	± 1.7	22.2	21.0×10^{-9}

NOTE. — Summary of results. For all stars the distance and $N(\text{H I})$ is given. We list for the detections, the observed equivalent widths of the Ca II Kline, and the resulting Ca II abundance. For non-detections, we give the predicted Ca II K equivalent width before and after taking into account the safety factors. The significance of the non-detections is given as the ratio of $W_{\lambda, \text{saf}}/\sigma(W_{\lambda})$.

scope Array (ATA) for our sightlines.

Complex C shows little evidence of dust depletion (Collins et al. 2003), so we do not take into account depletion effects. In the ideal case, the gas-phase abundance towards the stellar sightline will be known, from measurements of nearby extra-galactic sightlines. This is the case for S441, which is very close ($< 0.5^\circ$) to the Mrk 290 sightline. For the S135 and S139 sightlines, however, we must into account possible variations in gas metallicity and ionization conditions. Since Ca II is not the dominant ionization stage of Ca in the ISM and HVCs (IP = 11.9 eV; Morton 2003), a safety factor of $2\times$ is included to account for this (Wakker 2001). Several authors have shown evidence that the metallicity of Complex C varies from QSO sightline to sightline in the range $0.1 - 0.3 Z_\odot$, independent of ionization effects (e.g. Gibson et al. 2001; Collins et al. 2007). This may be a result of Complex C mixing with local, enriched gas (Gibson et al. 2001; Tripp et al. 2003). Ca II abundances have been measured toward only two sightlines: Mrk 290 [$A(\text{Ca II}) = 21 \times 10^{-9}$] and PG 1351+640 [$A(\text{Ca II}) = 18 \times 10^{-9}$] (Wakker et al. 1996; Wakker 2001). Mrk 290 is closest to the S135 and S139 sightlines, so we adopt the measured abundance, and include a safety factor of $3\times$, in line with the metallicity variations.

Table 2 shows that even under pessimistic assumptions, the excellent quality of the Keck data gives us confidence in our non-detections. Using the H I data from the LAB survey, we infer the gas-phase Ca II abundance $A(\text{Ca II}) = N(\text{Ca II})/N(\text{H I})$ for our two detections. Both sightlines give similar results, which are also in good agreement with the values observed towards Mrk 290 and PG 1351+640, up to 20 degrees away. Such good agreement seems to imply that there are not large variations of the Ca II abundance across the cloud, which further strengthens the case for our non-detections providing lower distance limits. Adopting Ca II abundances from the relation of Wakker & Mathis (2000), which predicts $A(\text{Ca II})$ as a function of $N(\text{H I})$, does not affect our conclusions.

All our distance limits imply a canonical distance of 10 ± 2.5 kpc to Complex C in the higher latitude regions. Towards S674 at the highest longitudes, the HVC is con-

strained to be closer than 10.4 ± 2.6 kpc. In the middle latitudes, both the upper limit from S437 ($d < 11.3 \pm 2.8$ kpc) and lower set by S441 ($d > 10.2 \pm 2.6$ kpc) are consistent with the 10 kpc distance. At lower latitudes, we have only lower limits from S135 ($d > 12.8 \pm 3.2$ kpc) and S139 ($d > 7.8 \pm 2.0$ kpc). While both these stars are consistent with a 10 kpc distance for Complex C, we do not have an upper limit for the low latitude parts of the complex, and cannot exclude the possibility of a distance gradient. It would not be surprising if such a distance gradient existed given the large angular size of Complex C. Observations at high latitudes of closer stars in the range 6–8 kpc, and more distant stars in the lower longitude, lower latitude regions, are needed to substantiate this speculation. We stress that the $\sim 25\%$ distance accuracy is the current limit of stellar classification techniques for horizontal-branch stars, and applies to *all* results; a systematic calibration effort is required to reduce this uncertainty.

4. DISCUSSION

For ease of discussion, we first consider Complex C to be at a uniform distance of 10 kpc. With such a large projected size, this is unlikely unless Complex C has a curved geometry. Using the total flux for Complex C (Wakker & van Woerden 1991), our distance limit implies a mass for Complex C of $M_{\text{H I}} = 4.9^{+2.8}_{-2.2} \times 10^6 M_\odot$. To calculate the total mass, we include a factor of 1.4 to account for helium, and an ionization fraction $M_{\text{H}+} = 0.18 M_{\text{H I}}$ (Wakker et al. 1999; Sembach et al. 2003). Since there is no indication of molecular gas (Murphy et al. 2000; Richter et al. 2001), we take $M_{\text{H}} = M_{\text{H}+} + M_{\text{H I}}$, and derive a total mass for Complex C of $M_{\text{tot}} = 8.2^{+4.6}_{-2.6} \times 10^6 M_\odot$.

At $\sim 5 \times 10^6 M_\odot$, Complex C has an H I mass of order the mass that Lockman (2003) derived for Complex H by assuming that it is a satellite of the MW merging with the outer disk. Of the recently discovered low-luminosity dwarf galaxies recently discovered in the SDSS (e.g. Willman et al. 2005a,b; Belokurov et al. 2006, 2007), only Leo T has been shown to have associated neutral gas (Ryan-Weber et al. 2007); the H I mass of Complex C is more than an order of magnitude more than that of Leo T, and is comparable to other local group dwarf ir-

regulars, such as Pegasus, DDO 210 and LGS 3 (Mateo 1998). Complex C is also an order of magnitude more massive than the HVCs surrounding the M31/M33 system (Westmeier et al. 2005). Despite the large masses of neutral gas, a variety of searches have failed to find any evidence for an associated stellar content with any HVC (e.g. Willman et al. 2002; Simon & Blitz 2002; Siegel et al. 2005; Simon et al. 2006), and there is no evidence of a connection between Complex C and any dwarf galaxies.

The calculation of the mass flux onto the Galaxy that Complex C provides is hampered by our ignorance of the tangential velocity, which limits our ability to determine the vertical velocity with respect to the disk. We attempt to average over much of our ignorance by considering the average mass flow over the whole accretion timescale (i.e. the time it takes for the whole complex to accrete). The furthest gas from the plane, at highest latitudes is that between $b = 55 - 60$ deg—we choose a representative direction $(l, b) = (120 \text{ deg}, 58 \text{ deg})$. At $d = 10$ kpc, this gas is ~ 8 kpc above the disk, and has a line-of-sight velocity $v_{\text{LSR}} = -126 \text{ km s}^{-1}$. To remove the disk rotation, we convert to “deviation velocity”, which is the amount by which the gas deviates from a model of Galactic rotation (de Heij et al. 2002), giving $v_{\text{dev}} = -105 \text{ km s}^{-1}$. A range of vertical velocities is allowed by the projection of the line-of-sight velocity into the vertical, and the unknown tangential component. Given the uncertainties, we simply take $v_z = -100 \text{ km s}^{-1}$, yielding an accretion timescale $\sim 80 \text{ Myr}$, and a mass flux of order $\sim 0.1 \text{ M}_{\odot} \text{ yr}^{-1}$. It is worth noting that Tripp et al. (2003) have argued that the lower latitude parts of Complex C show signs of interaction with the thick disk or lower halo.

The condensing cloud model (Sommer-Larsen 2006; Peek et al. 2007) predicts $\sim 0.2 \text{ M}_{\odot} \text{ yr}^{-1}$ of accretion coming from HVCs. Meanwhile, chemical evolution models require such infall to reproduce the observed metallicity distribution in the disk (Alibés et al. 2001; Fenner & Gibson 2003). The most recent calculations suggest an infall rate of $\sim 1 \text{ M}_{\odot} \text{ yr}^{-1}$ about 5 Gyr ago, falling roughly half that at the present epoch (Chiappini et al. 2001). Given the uncertainties involved, we can say only that the measured mass flux is broadly consistent with both these predictions.

5. CONCLUSION

We have used the presence and absence of Ca II K absorption in 5 stars aligned with the high-velocity cloud Complex C to derive a distance to the complex of 10 ± 2.5 kpc. At high latitude, we detect HVC gas in absorption towards stars ~ 10 and ~ 11 kpc away, setting upper distance limits. At similar latitudes, a non-detection provides a lower limit of ~ 10 kpc. Non-detections in stars at ~ 8 and ~ 13 kpc at lower latitudes are consistent with this distance. Since the stellar distances are accurate to $\sim 25\%$, a canonical distance of 10 ± 2.5 kpc is set, but we cannot exclude the possibility of a distance gradient, which would mean larger distances for lower latitude parts of Complex C. Indeed, such a distance gradient would be expected based on the large angular size of the complex, but the currently available limits are insufficient to derive a useful distance gradient.

The distance implies an H I mass for Complex C of $M_{\text{HI}} = 4.9^{+2.8}_{-2.2} \times 10^6 \text{ M}_{\odot}$. Applying corrections for helium and ionized gas yields total mass of $M_{\text{tot}} = 8.2^{+4.6}_{-2.6} \times 10^6 \text{ M}_{\odot}$. We derive a mass inflow rate of $\sim 0.1 \text{ M}_{\odot} \text{ yr}^{-1}$, which is broadly consistent with predictions from condensing cloud model, and chemical evolution models of the Galaxy. Our accurate distance contributes to a picture in which the large HVC complexes are nearby Galactic objects. Complexes for which stellar distances have been determined are all within $d < 10 - 15$ kpc (van Woerden et al. 1999; Thom et al. 2006; Wakker et al. 2007a,b). With the first elements to a solution to the high-velocity cloud distance problem now well established, continuing efforts will provide a more complete census of neutral gas in the Milky Way halo.

We thank Tobias Westmeier for providing the HVC data from which Figure 7 was made, and for the Effelsberg spectrum towards S441. This work has made use of the NIST Atomic Spectra Database (v3.1), available online at <http://physics.nist.gov/asd3>. C.T. acknowledges partial support from NASA through the American Astronomical Society’s Small Research Grant Program, and NASA grant NNG06GC36G. C.H. acknowledges support from NSF grant AST-0406987.

REFERENCES

- Alibés, A., Labay, J., & Canal, R. 2001, *A&A*, 370, 1103
 Belokurov, V., Zucker, D. B., Evans, N. W., Kleya, J. T., Koposov, S., Hodgkin, S. T., Irwin, M. J., Gilmore, G., Wilkinson, M. I., Fellhauer, M., Bramich, D. M., Hewett, P. C., Vidrih, S., De Jong, J. T. A., Smith, J. A., Rix, H.-W., Bell, E. F., Wyse, R. F. G., Newberg, H. J., Mayeur, P. A., Yanny, B., Rockosi, C. M., Gnedin, O. Y., Schneider, D. P., Beers, T. C., Barentine, J. C., Brewington, H., Brinkmann, J., Harvanek, M., Kleinman, S. J., Krzesinski, J., Long, D., Nitta, A., & Snedden, S. A. 2007, *ApJ*, 654, 897
 Belokurov, V., Zucker, D. B., Evans, N. W., Wilkinson, M. I., Irwin, M. J., Hodgkin, S., Bramich, D. M., Irwin, J. M., Gilmore, G., Willman, B., Vidrih, S., Newberg, H. J., Wyse, R. F. G., Fellhauer, M., Hewett, P. C., Cole, N., Bell, E. F., Beers, T. C., Rockosi, C. M., Yanny, B., Grebel, E. K., Schneider, D. P., Lupton, R., Barentine, J. C., Brewington, H., Brinkmann, J., Harvanek, M., Kleinman, S. J., Krzesinski, J., Long, D., Nitta, A., Smith, J. A., & Snedden, S. A. 2006, *ApJ*, 647, L111
 Bregman, J. N. 1980, *ApJ*, 236, 577
 Chiappini, C., Matteucci, F., & Romano, D. 2001, *ApJ*, 554, 1044
 Collins, J. A., Shull, J. M., & Giroux, M. L. 2003, *ApJ*, 585, 336
 —. 2007, *ApJ*, 657, 271
 Danly, L., Albert, C. E., & Kuntz, K. D. 1993, *ApJ*, 416, L29+
 de Avillez, M. A. 2000, *Ap&SS*, 272, 23
 de Heij, V., Braun, R., & Burton, W. B. 2002, *A&A*, 391, 159
 Dorman, B. 1992, *ApJS*, 81, 221
 Fenner, Y. & Gibson, B. K. 2003, *Publ. Astr. Soc. Aus.*, 20, 189
 Fox, A. J., Savage, B. D., Wakker, B. P., Richter, P., Sembach, K. R., & Tripp, T. M. 2004, *ApJ*, 602, 738
 Gibson, B. K., Giroux, M. L., Penton, S. V., Stocke, J. T., Shull, J. M., & Tumlinson, J. 2001, *AJ*, 122, 3280
 Girardi, L., Grebel, E. K., Odenkirchen, M., & Chiosi, C. 2004, *A&A*, 422, 205
 Haffner, L. M., Reynolds, R. J., Tufte, S. L., Madsen, G. J., Jaehnig, K. P., & Percival, J. W. 2003, *ApJS*, 149, 405
 Houck, J. C. & Bregman, J. N. 1990, *ApJ*, 352, 506

- Hulsbosch, A. N. M. & Raimond, E. 1966, *Bull. Astron. Inst. Netherlands*, 18, 413
- Kalberla, P. M. W., Burton, W. B., Hartmann, D., Arnal, E. M., Bajaja, E., Morras, R., & Pöppel, W. G. L. 2005, *A&A*, 440, 775
- Kaufmann, T., Mayer, L., Wadsley, J., Stadel, J., & Moore, B. 2006, *MNRAS*, 370, 1612
- Lee, Y.-S., Beers, T. C., Sivarani, T., Johnson, J., An, D., Wilhelm, R., Allende-Prieto, C., Fiorentin, P. R., Bailer-Jones, C. A., Norris, J. E., Yanny, B., Rockosi, C. M., Newberg, H. J., Cudworth, K. M., & Pan, K. 2008, *ApJ*, submitted
- Lockman, F. J. 2003, *ApJ*, 591, L33
- Maller, A. H. & Bullock, J. S. 2004, *MNRAS*, 355, 694
- Mateo, M. L. 1998, *ARA&A*, 36, 435
- Mathewson, D. S., Cleary, M. N., & Murray, J. D. 1974, *ApJ*, 190, 291
- Meggers, W. F., Corliss, C. H., & Scribner, B. F. 1976 (National Bureau of Standards Monograph 145, Washington: US Government Printing Office (USGPO), 1975)
- Morton, D. C. 2003, *ApJS*, 149, 205
- Muller, C. A., Oort, J. H., & Raimond, E. 1963, *Comptes Rendus de l'Académie des Sciences Paris*, 257, 1661
- Murphy, E. M., Sembach, K. R., Gibson, B. K., Shull, J. M., Savage, B. D., Roth, K. C., Moos, H. W., Green, J. C., York, D. G., & Wakker, B. P. 2000, *ApJ*, 538, L35
- Oort, J. H. 1966, *Bull. Astron. Inst. Netherlands*, 18, 421
- Oosterloo, T., Fraternali, F., & Sancisi, R. 2007, *AJ*, 134, 1019
- Pagel, B. E. J. & Patchett, B. E. 1975, *MNRAS*, 172, 13
- Peek, J. E. G., Putman, M. E., & Sommer-Larsen, J. 2007, *ArXiv e-prints*, 705
- Putman, M. E., Staveley-Smith, L., Freeman, K. C., Gibson, B. K., & Barnes, D. G. 2003, *ApJ*, 586, 170
- Putman, M. E., Thom, C., Gibson, B. K., & Staveley-Smith, L. 2004, *ApJ*, 603, L77
- Richter, P., Sembach, K. R., Wakker, B. P., & Savage, B. D. 2001, *ApJ*, 562, L181
- Ryan-Weber, E. V., Begum, A., Oosterloo, T., Pal, S., Irwin, M. J., Belokurov, V., Evans, N. W., & Zucker, D. B. 2007, *MNRAS*, in press (arXiv:0711.2979)
- Ryans, R. S. I., Keenan, F. P., Sembach, K. R., & Davies, R. D. 1997, *MNRAS*, 289, 83
- Schwarz, U. J., Wakker, B. P., & van Woerden, H. 1995, *A&A*, 302, 364
- Sembach, K. R. & Savage, B. D. 1992, *ApJS*, 83, 147
- Sembach, K. R., Wakker, B. P., Savage, B. D., Richter, P., Meade, M., Shull, J. M., Jenkins, E. B., Sonneborn, G., & Moos, H. W. 2003, *ApJS*, 146, 165
- Siegel, M. H., Majewski, S. R., Gallart, C., Sohn, S. T., Kunkel, W. E., & Braun, R. 2005, *ApJ*, 623, 181
- Simon, J. D. & Blitz, L. 2002, *ApJ*, 574, 726
- Simon, J. D., Blitz, L., Cole, A. A., Weinberg, M. D., & Cohen, M. 2006, *ApJ*, 640, 270
- Sirko, E., Goodman, J., Knapp, G. R., Brinkmann, J., Ivezić, Ž., Knerr, E. J., Schlegel, D., Schneider, D. P., & York, D. G. 2004, *AJ*, 127, 899
- Sommer-Larsen, J. 2006, *ApJ*, 644, L1
- Thom, C. 2006, PhD thesis, Swinburne University of Technology
- Thom, C., Putman, M. E., Gibson, B. K., Christlieb, N., Flynn, C., Beers, T. C., Wilhelm, R., & Lee, Y. S. 2006, *ApJL*, 638, L97
- Tripp, T. M., Wakker, B. P., Jenkins, E. B., Bowers, C. W., Danks, A. C., Green, R. F., Heap, S. R., Joseph, C. L., Kaiser, M. E., Linsky, J. L., & Woodgate, B. E. 2003, *AJ*, 125, 3122
- Tufte, S. L., Reynolds, R. J., & Haffner, L. M. 1998, *ApJ*, 504, 773
- van Woerden, H., Schwarz, U. J., Peletier, R. F., Wakker, B. P., & Kalberla, P. M. W. 1999, *Nature*, 400, 138
- Wakker, B. P. 2001, *ApJS*, 136, 463
- Wakker, B. P., Howk, J. C., Savage, B. D., van Woerden, H., Tufte, S. L., Schwarz, U. J., Benjamin, R., Reynolds, R. J., Peletier, R. F., & Kalberla, P. M. W. 1999, *Nature*, 402, 388
- Wakker, B. P., Kalberla, P. M. W., van Woerden, H., de Boer, K. S., & Putman, M. E. 2001, *ApJS*, 136, 537
- Wakker, B. P. & Mathis, J. S. 2000, *ApJ*, 544, L107
- Wakker, B. P., Oosterloo, T. A., & Putman, M. E. 2002, *AJ*, 123, 1953
- Wakker, B. P. & van Woerden, H. 1991, *A&A*, 250, 509
- Wakker, B. P., van Woerden, H., Schwartz, U. J., Peletier, R. F., & Douglas, N. G. 1996, *A&A*, 306, L25+
- Wakker, B. P., York, D. G., Howk, J. C., Barentine, J. C., Wilhelm, R., Peletier, R. F., van Woerden, H., Beers, T. C., Ivezić, Ž., Richter, P., & Schwarz, U. J. 2007a, *ApJ*, 670, L113
- Wakker, B. P., York, D. G., Wilhelm, R., Barentine, J. C., Richter, P., Beers, T. C., Ivezić, Ž., & Howk, J. 2007b, *ApJ* submitted (arXiv:0709.1926)
- Westmeier, T., Braun, R., & Thilker, D. 2005, *A&A*, 436, 101
- Wilhelm, R., Beers, T. C., & Gray, R. O. 1999, *AJ*, 117, 2308
- Willman, B., Blanton, M. R., West, A. A., Dalcanton, J. J., Hogg, D. W., Schneider, D. P., Wherry, N., Yanny, B., & Brinkmann, J. 2005a, *AJ*, 129, 2692
- Willman, B., Dalcanton, J., Ivezić, Ž., Schneider, D. P., & York, D. G. 2002, *AJ*, 124, 2600
- Willman, B., Dalcanton, J. J., Martinez-Delgado, D., West, A. A., Blanton, M. R., Hogg, D. W., Barentine, J. C., Brewington, H. J., Harvanek, M., Kleinman, S. J., Krzesinski, J., Long, D., Neilsen, Jr., E. H., Nitta, A., & Snedden, S. A. 2005b, *ApJ*, 626, L85